A universal biocompatible coating for enhanced lubrication and bacterial inhibition†

Di Suo, Jingdong Rao, Haimang Wang,b Ziheng Zhang, Polly Hang-Mei Leung, Hongyu Zhang, Xiaoming Tao and Xin Zhao

Antibacterial coatings that inhibit bacterial adhesion are essential for many implanted medical devices. A variety of antibacterial strategies, such as repelling or killing bacteria, have been developed, but not yet been completely successful. Here, we develop a universal biocompatible coating for enhanced lubrication and bacterial inhibition. The coating is designed based on mussel-inspired surface-attachable dopamine bases and consists of lubricating zwitterionic polymers poly(2-methacryloxyethyl phosphorylcholine) (MPC) and a bacterial membrane destroying anti-bacteria molecule poly(3-hydroxybutyric acid) (PHB). The coating boasts strong adhesion to surfaces of various materials (such as polydimethylsiloxane (PDMS)/ceramic/316L stainless steel (316L SS); it is biocompatible, and cell/platelet/bacteria repelling, significantly inhibiting bacterial growth. We envision that our strategy represents a universal strategy for surface functionalization of a variety of biomedical devices and implants.

Introduction

Medical implants and devices have been designed for a variety of therapeutic and rehabilitative uses, such as joint replacement implants, pacemakers and endovascular stents. (1) During the medical intervention or implantation, protein adhesion on the surface of biomaterials occurs immediately, (2) which may cause adhesion of microorganisms and formation of biofilms on the implant surfaces. (3) To circumvent this problem, many studies have been conducted by using antimicrobial agents/ materials (e.g., silver ions, silver/gold nanoparticles, antibiotics and antimicrobial peptides) as components in biomedical implants. (4–6) However, the drug resistance, difficulty for metallic nanoparticles to metabolize and degrade, and/or the potential toxicity of the antibacterial agents limit the further development. (7) Meanwhile, although the bacteria can be killed by anti-bacterial molecules, the accumulation of dead bacteria and its debris hides the bactericidal active sites and reduces the anti-bacterial effect for the later adherent bacteria, triggering an immune or inflammatory response and compromising the treatment efficacy. (8–10) Moreover, implant debris caused by the interfacial micro-motion and abrasion is also a major concern to widespread inflammation and necrosis. (11)

To tackle this, zwitterionic polymers have been used to modify surfaces of biomedical implants. (12) Zwitterionic polymers have one positively charged and one negatively charged group on the same repeating unit; it can strongly bind to water through electrostatically induced hydration and can decrease friction and wear once grafted onto a substance surface (e.g., metal, polymer, ceramic). (13–16) It has been widely used for fabricating antifouling surfaces on biomedical materials and devices. (17) Although lubrication can remove bacteria to certain extent, it cannot eliminate all bacteria to prevent infection due to the strong proteinaceous extracellular appendages of some bacteria. (18) This makes the physical antimicrobial properties of zwitterionic coatings insufficient to address clinical anti- microbial needs as the remaining bacteria may lead to the recurrence of infection. To improve lubrication and resist bacterial infection simultaneously, a universal coating with lubricating and bacteria resisting properties is highly sought after.

In this study, we developed a universal dopamine-based poly(2-methacryloxyethyl phosphorylcholine) (MPC) and poly (3-hydroxybutyric acid) (PHB) co-deposited terpolymer coating (DMA–MPC–PHB) to modify different material surfaces including metal, polymer and ceramic (Zirconia). MPC has a positive group ($N^+(CH)$) and a negative group (PO^{3-}) that mimics the 334 charged phosphatidylcholine lipids in articular cartilage, with highly effective lubrication ability. (16) PHB is a bio-synthesized and biodegradable microbial-based biopolymer, which can effectively destroy biofilms by disrupting cell walls or membranes. 19,20 Moreover, PHB possesses broad-spectrum antibacterial ability: it can inhibit both Gram-positive and negative bacteria, and even induce the death of fungus. (19) The combination of PHB and MPC is expected to endow the medical implants/devices with both improved lubrication and anti-bacteria ability. Dopamine methacrylamide (DMA), a type of dopamine rich in double bonds, was used as basement material, where MPC and PHB could be connected onto it by addition reaction of carbon–carbon double bond in the presence of the initiator azodiisobutyronitrile (AIBN) (Fig. 1). We found that the DMA–MPC–PHB coating could significantly inhibit cell adhesion, blood coagulation and bacteria growth. We envision that our strategy can inspire design of surface functionalization of a wide range of biomedical devices or implants.

Results and discussion

Synthesis and optimization of DMA–MPC–PHB coating

The terpolymer DMA–MPC–PHB was composed of a synthetic anchoring molecular DMA, a lubrication agent MPC and an antibacterial element PHB. To screen suitable constitution of DMA–MPC–PHB for better lubrication and antibacterial effect, four different proportions of terpolymers were prepared. DMA– MPC–PHB with the mass ratio of 1:1:1, 1:1:2, 1:2:1 and 1 : 2 : 2 (denoted as DMA–MPC–PHB-1, DMA–MPC–PHB-2, DMA–MPC–PHB-3, DMA–MPC–PHB-4, respectively) were synthesized by free radical polymerization in the presence of initiator AIBN. We then characterized the chemical properties of the resultant DMA–MPC–PHB coating. Fig. S1† showed the FTIR spectra of four kinds of DMA–MPC–PHB terpolymer, where the characteristic peak belonged to DMA ($\sim$1400–1600 cm^{-1}), PvO peak ($\sim$1244 cm^{-1}) and P–O peak ($\sim$960–1060 cm^{-1}) belonged to MPC, and ester carbonyl peak ($\sim$1720–1740 cm^{-1}) belonged to PHB. The above results indicate successful synthesis of DMA–MPC–PHB.

To optimize the formulations of DMA–MPC–PHB, we characterized the hydrophilicity of the terpolymers coated onto the surface of 316L stainless steel (316L SS) substrate by water contact angle (WCA) analysis. (21) The data (Fig. S2A†) proved the surface modification greatly decreased the WCA from 88.2° for bare 316L SS to 32.5°, 33.1°, 22.8° and 18.7° for the DMA– MPC–PHB-1, DMA–MPC–PHB-2, DMA–MPC–PHB-3, and DMA–MPC–PHB-4 coatings respectively, indicating increasing hydrophilicity. Furthermore, the antibacterial experiment (Fig. S2B and 2C†) demonstrated that the DMA–MPC–PHB coatings could significantly inhibit bacteria growth with decreased bacterial colonies compared with bare 316L SS group (confluent bacterial growth). The above results have demonstrated that the DMA–MPC–PHB-4 terpolymer had the best hydrophilic effect: they had decreased WCA by 4.72-fold, 1.74-fold, 1.77-fold and 1.22-fold compared to 316L SS, DMA– MPC–PHB-1, DMA–MPC–PHB-2 and DMA–MPC–PHB-3, respectively; and DMA–MPC–PHB-4 showed nearly no bacterial colony, indicating excellent lubrication and antibacterial effect. DMA–MPC–PHB-4 terpolymer with the ratio 1 : 2 : 2 was thus used in subsequent experiments.

Fabrication of DMA–MPC–PHB coating on different substrates

As dopamine and its derivatives can serve as intercalators to effectively promote the self-adhesive coating process by covalent bond and noncovalent bond interactions, (22) the optimal DMA–MPC–PHB-4 was then applied to modify the 316L SS, polydimethylsiloxane (PDMS) and ceramic (Zirconia) substrate. 316L SS,

PDMS and ceramic are selected as they are the most widely used medical materials. 316L SS is the raw material for cardiovascular stents and other surgical instruments, and PDMS is usually utilized as medical tube which provides fluids (such as blood and urine) and gas circulation, while ceramic is often used in the construction of bone scaffolds, artificial joints, artificial teeth, etc. Fig. 2A showed (1) H nuclear magnetic resonance (NMR) spectrum of DMA– MPC–PHB-4. The signals at 7.87 and 8.87 ppm belonged to DMA, the signal at 3.16 ppm was assigned to MPC, while 2.51 ppm signal corresponded to the characteristic group of PHB. Then, X-ray photoelectron spectroscopy (XPS) was used to investigate the chemical element compositions on each substrate surfaces. Fig. 2B showed the bare samples only had substrate materials' peak (Fe 2p in 316L SS, Si 2P in PDMS and Zr 3d in ceramic), while the coated samples possessed both the substrate materials' peak and obvious N 1s peak (403.8 eV) and P 2p peak (134.8 eV). The high-resolution narrow spectra (Fig. S3A†) exhibited one strong P peak in each coated groups, and N 1s was separated into two types, which corresponded to amide group ($-NHCO^-$, bending energy 400.8 eV) in DMA and quaternary ammonium group ($-N^+(CH3)^3$, bending energy 403.7 eV) in MPC. Then FTIR spectra were further used to analyze the chemical structure of each coating. Fig. 2C showed there were obvious –CH2 peak (~3000 cm^{-1}), –CvC peak (~1600 cm^{-1}), benzene ring peak (~1400 cm^{-1}), –PvO (~1244 cm^{-1}) and –P–O peak ($\sim 960-1060$ cm^{-1}) in the coated samples. Meanwhile, the FTIR spectra of all coated samples displayed similar distribution, possessed same characteristic peaks of DMA–MPC–PHB, suggesting our developed coating could indistinguishably attach to these three materials. The deposition of DMA–MPC–PHB coating was also evidenced by the coating thickness of 31 ± 3 nm on 316L SS, 27 ± 4 nm on PDMS and 43 ± 3 nm on the ceramic surface using a surface profiler. Furthermore, the surface morphology of each sample was observed by scanning electron microscopy (SEM) (Fig. S3B†). Compared with the smooth bare surface, the coated samples possessed uniform small protuberances and formed a film alike appearance. These above results proved that DMA–MPC–PHB has been successfully modified onto 316L SS, PDMS and ceramic substrates, suggesting the universality of the DMA–MPC–PHB coating.
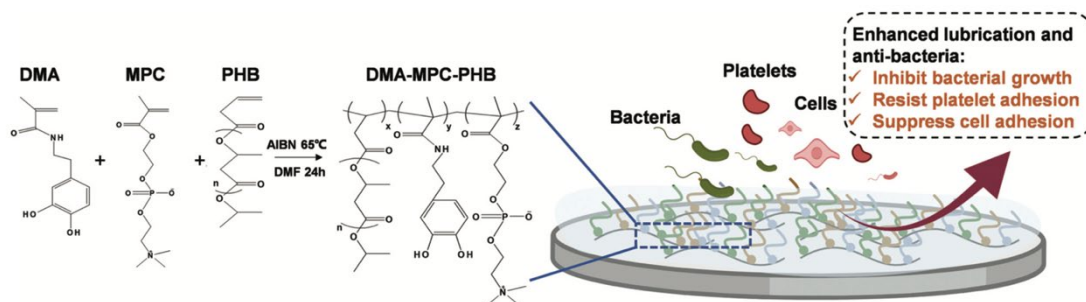

Fig. 1 Illustration of the fabrication and function of DMA–MPC–PHB coating. Synthesis of DMA–MPC–PHB coating (left) and enhanced lubrication and anti-bacterial effect of DMA–MPC–PHB coating for bacterial inhibition, and platelet/cell repelling (right).
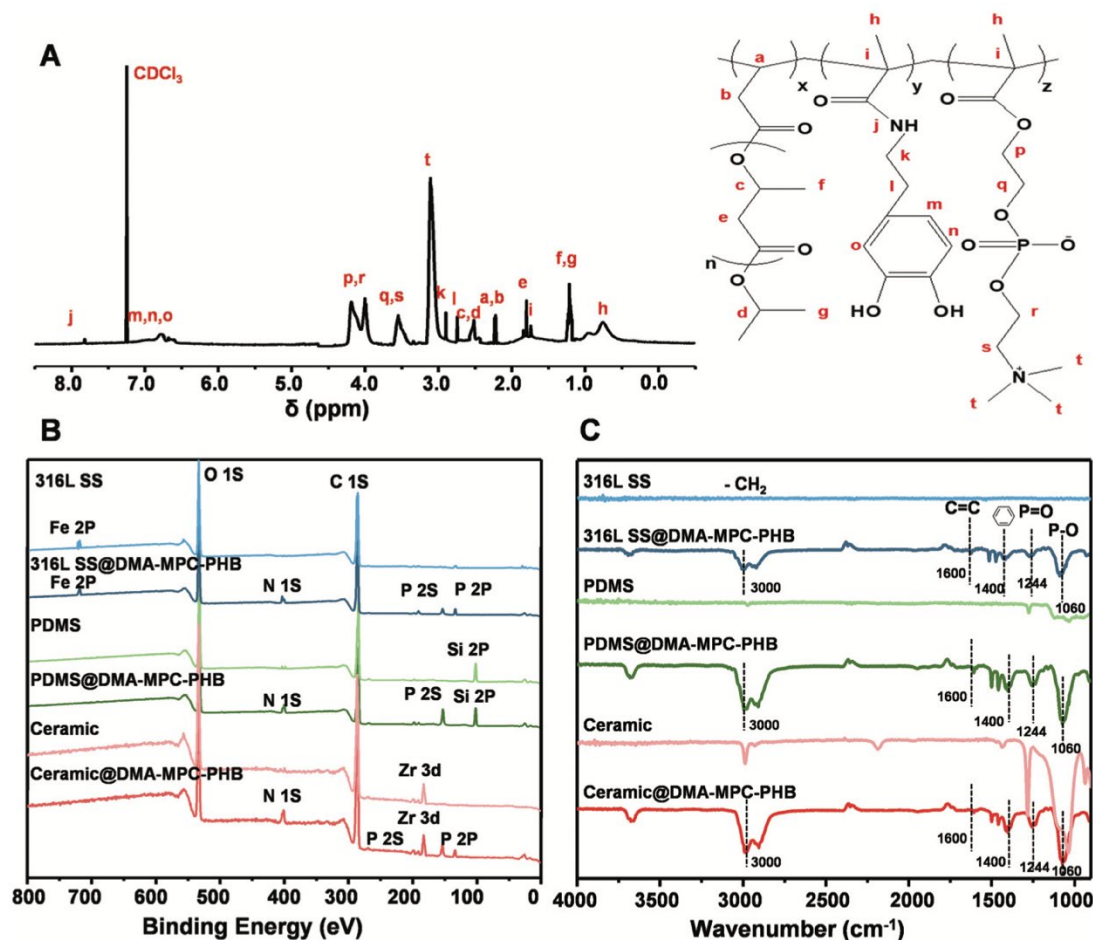
Fig. 2 Chemical characterization of the DMA–MPC–PHB terpolymer coating. (A) ^{1}H NMR spectrum of DMA–MPC–PHB terpolymer. (B) XPS spectra of bare and terpolymer-coated 316L SS/PDMS/ceramic. (C) FTIR spectra of bare and terpolymer-coated 316L/PDMS/ceramic.

Lubrication performance of DMA–MPC–PHB coating

The lubrication test was carried out to characterize the lubrication effect of the DMA–MPC–PHB terpolymer-coated 316L SS, PDMS and ceramic using atomic force microscope (AFM). Fig. 3A showed the schematic diagram of the experimental device of the lubrication test: polytetrafluoroethylene (PTFE) pin was used to test the coefficient of friction (COF) of the surface when applying different load pressure onto the holder and rubbing back and forth.[23] Fig. 3B–D displayed the COF data of the bare and the coated samples at different loads. With the load increasing, the COF of the bare material ascended gradually, from 0.207 to 0.359 in 316L SS, 0.135 to 0.159 in PDMS and 0.362 to 0.559 in ceramic, indicating the increased friction. On the contrary, after modification with DMA–MPC–PHB-4 coating, significant decrease of COF was observed. Under the highest load (300 nN), COF value declined from 0.359 to 0.213 in 316L SS (decrease by 40.67%), from 0.159 to 0.093 in PDMS (decrease by 41.51%) and from 0.559 to 0.313 in ceramic (decrease by 44.01%). This suggested that the DMA–MPC–PHB-4 coating had excellent lubrication performance.
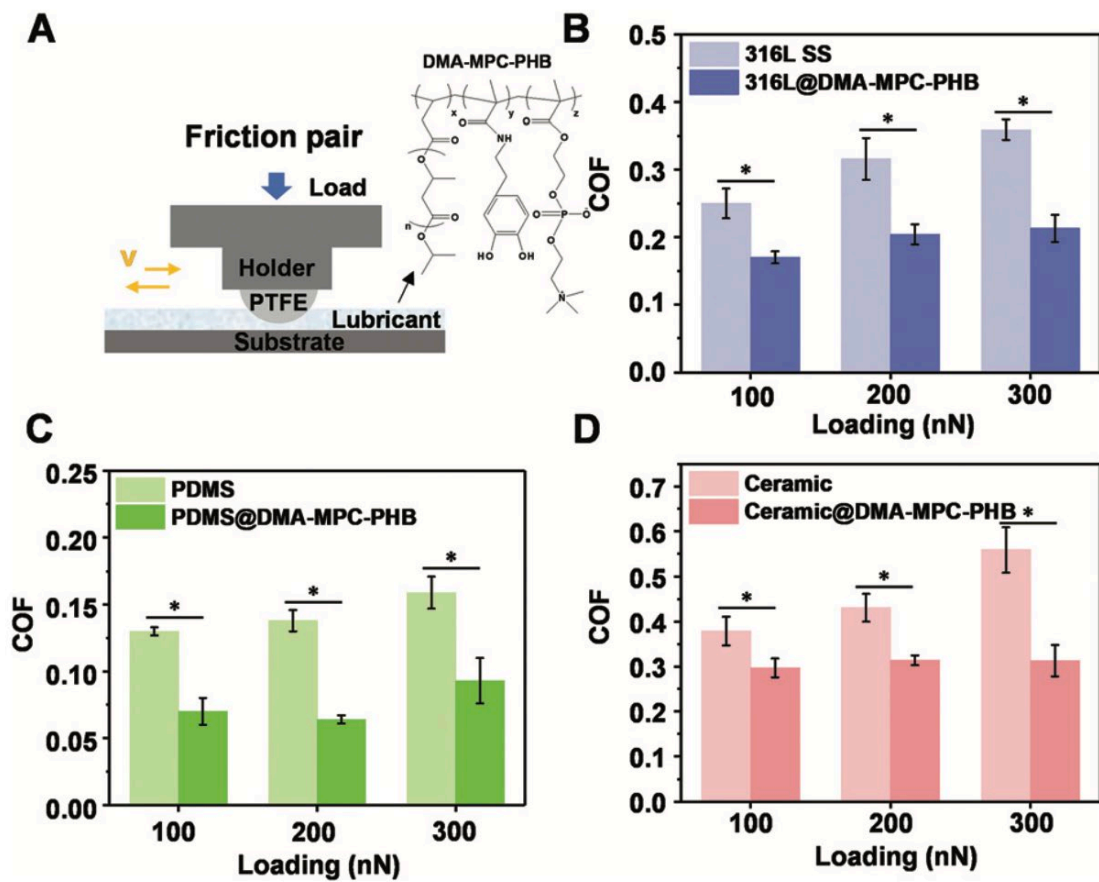
Fig. 3 Lubrication property of bare and terpolymer-coated 316L SS/ PDMS/ceramic. (A) Schematic diagram showing the experimental setup of the lubrication test. (B–D) Coefficient of friction (COF)-loading plots for the bare 316L SS/PDMS/ceramic or 316L/PDMS/ceramic@ DMA– MPC–PHB under different pressures of 100, 200, and 300 nN. Data are presented as mean ± SD and analysed by T-test, *p < 0.05 (DMA–MPC– PHB coated samples vs. bare surface).

To verify the decreased COF was related to the hydration lubrication mechanism of the DMA–MPC–PHB coating, WCA of each sample was evaluated. In Fig. S4,† the WCA of these three materials were all around 90°, showing the materials are highly hydrophobic. After surface modification, the WCA dramatically declined by almost 3-fold to 29.3°, 31.1° and 22.6° in the coated 316L SS, PDMS and ceramic surfaces, respectively, indicating the increased hydrophilicity. The elastohydrodynamic lubrication of DMA–MPC–PHB was attributed to the formation of a stable hydration by the zwitterionic charges ($-N^+(CH3)^3$ and $-PO4^{3-}$) in MPC, which could attach water owing to the electric dipole from residual charge oxygen atom and hydrogen atom of water molecules. (23) The hydration layer is able to resist high pressure without being destroyed, and it behaves as a fluid under the action of shear, enhancing the lubrication at the interface.24 Therefore, the above results demonstrated that the DMA–MPC–PHB-4 coating possessed excellent lubrication property, which has potential to reduce protein adhesion and inhibit cell/platelet/bacteria attachment.

Anti-bacterial performance of DMA–MPC–PHB coating

The initial adherence of bacteria to the surface is a critical factor in the creation of biofilms. Disrupting early colonization of bacteria is thus a key to reducing in vivo infection of biological materials. (25,26) To evaluate the anti-bacterial performance of the DMA–MPC–PHB-4 coating, bare substrates and DMA– MPC–PHB-4

coated samples were co-cultured with 1×10^6 Escherichia coli (E. coli) for 24 hours. Bacterial adhesion and its morphology were evaluated using SEM and quantified using the spread plate method, respectively. Fig. 4A1–F1 showed the colony images and the bacterial inhibition ratio (the specific ratio was derived from Fig. 4H) of bare substrates and DMA– MPC–PHB-4 coated substrates. Clearly, the bacterial inhibition ratios of all DMA–MPC–PHB-4 coated substrates were higher than 95%. The terpolymer coating of 316L SS had a bacterial inhibition ratio of even 98%. On the other hand, the bare substrates (Fig. 4A2–C2) suffered from severe bacterial adhesion, whereas only very few adherent bacteria were observed on the surface of DMA– MPC–PHB coated surfaces (Fig. 4D2–F2). Further result of spread plate counting of the bacteria indicated the density of 2.4×10^7, 2.5×10^7 and 2.7×10^7 CFU cm^{-2} for E. coli adhered to the bare 316L SS, PDMS and ceramic substrates, respectively (Fig. 4G). Bacterial adhesion was greatly reduced on the terpolymer coated surfaces. The density of E. coli attached to the DMA–MPC–PHB-4 coated surface was 8.2×10^5, 6.7×10^5 and 6.2×10^5 CFU cm^{-2}, which was two orders of magnitude less than the density of bacteria associated to bare substrates, showing that the terpolymer coating has good bacterial repulsion.
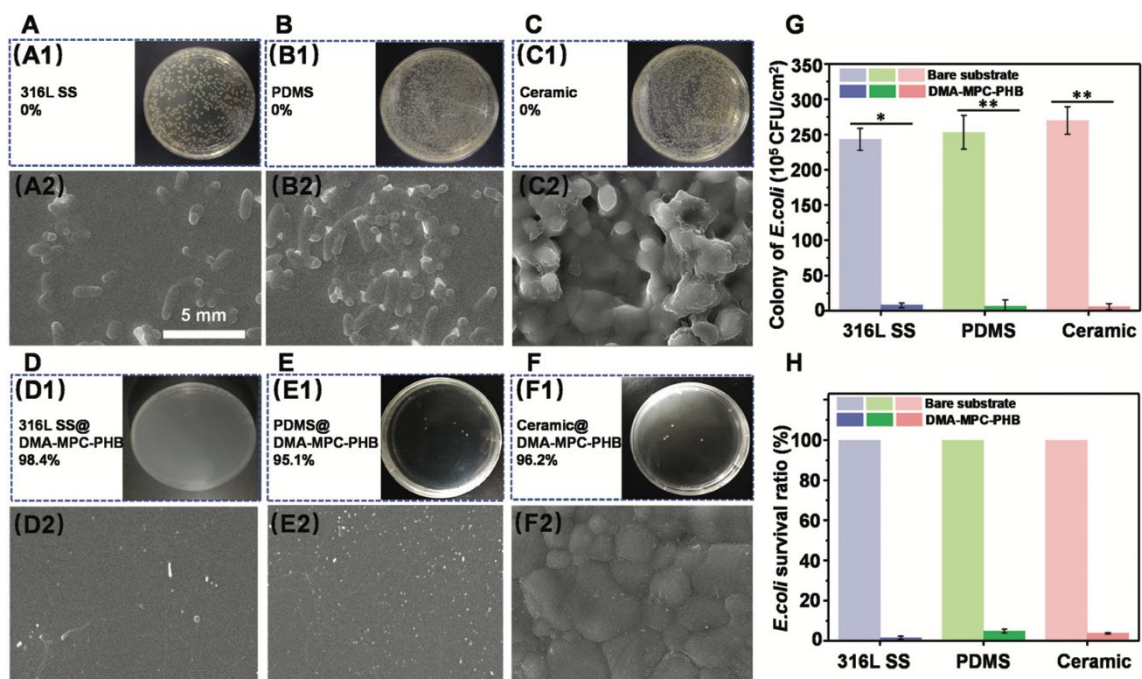

Fig. 4 Bacterial inhibition of bare and terpolymer-coated 316L SS/PDMS/ceramic. (A1–F1) The spread plate assay of bare and terpolymer-coated 316L/PDMS/ceramic substrates after culturing for 24 h. (A2–F2) SEM images showing E. coli adhesion on different substrates after culturing for 24 h. (G) The colony of E. coli on different substrates. (H) Bacterial survival ratio of the different substrates. Data are presented as mean ± SD and analysed by T-test, *p < 0.05, **p < 0.01 (DMA–MPC–PHB coated samples vs. bare surface).

Cytocompatibility of the DMA–MPC–PHB coating

To study the effect of DMA–MPC–PHB-4 coating on cell attachment, 3-day in vitro assessment was carried out. Initially, a similar number of human umbilical vein endothelial cells (HUVECs) was observed to attach to the surface of both bare and DMA–MPC–PHB-4-coated substrates. After 2 days of co-incubation, the cells dispersed well on the bare surface of 316L SS, PDMS, and ceramic sheets (Fig. 5A), while there were just a few cells attached to the DMA–MPC–PHB-4 coated surface. The density of cells attached to the coated surface was 1.1×10^4, 1.2×10^4 and 1.4×104 cm^{-2} after 48 hours of incubation, which was twice less than the density of the cells adhered to the bare substrates (Fig. 5B).

To further examine the cytocompatibility of the DMA–MPC– PHB-4 coating, HUVECs were seeded on cell plates, then the bare and coated samples were soaked into the medium and co-cultured with the cells for 48 hours. As seen in Fig. 5C, HUVECs co-cultured with DMA–MPC–PHB coatings exhibited the same viability as the bare group. After 48 hours, the cell viability was more than 90% on all bare and coated surfaces, suggesting that the DMA–MPC–PHB coating had no detrimental effect on cells and the cell adhesion resistance effect was owing to lubrication instead of cytotoxicity. These results revealed that the DMA–MPC–PHB coating could effectively reduce the cell adhesion, while being cytocompatible.
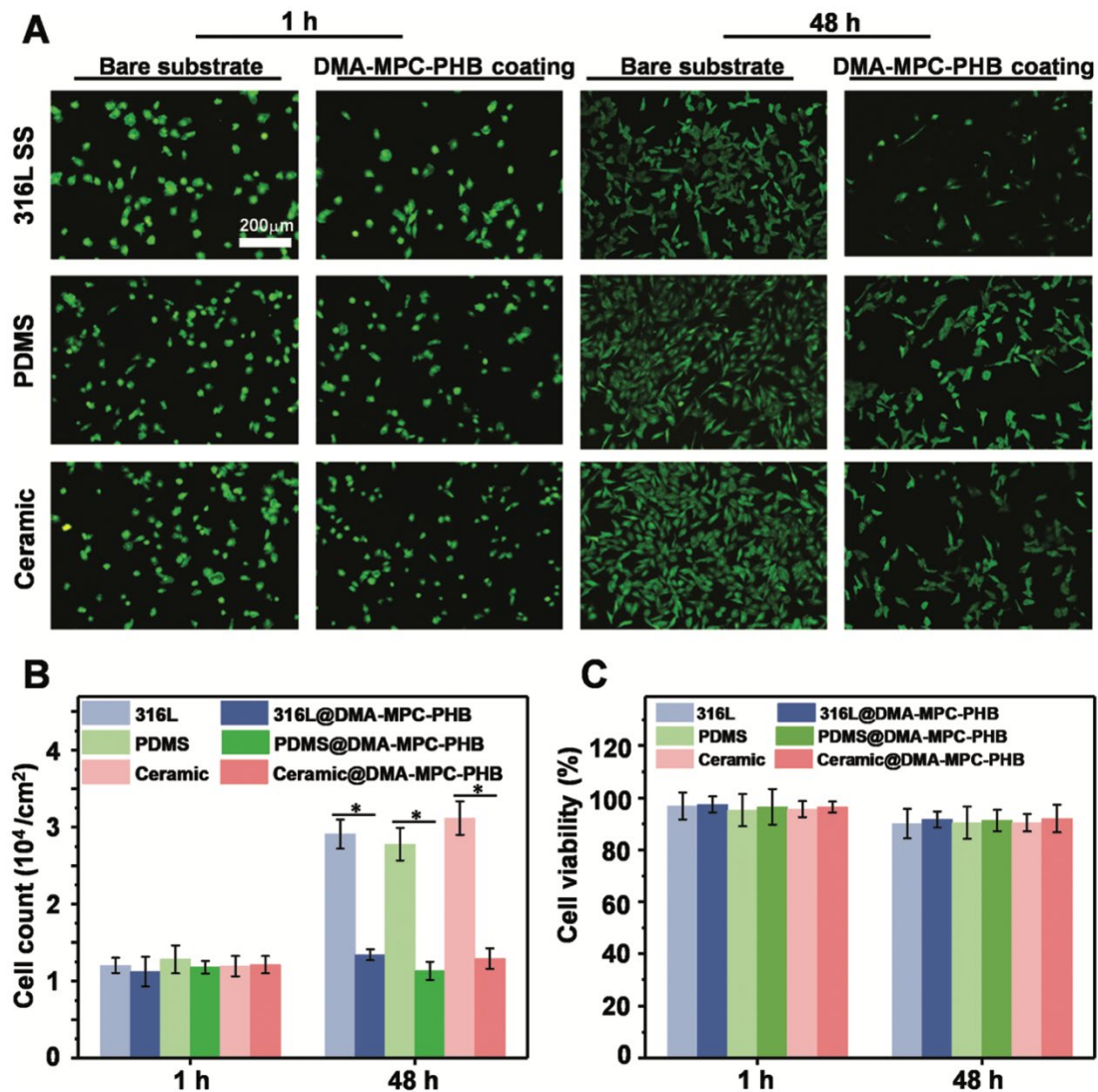

Fig. 5 Cell adhesion and potential cytotoxicity of bare and terpolymer-coated 316L SS/PDMS/ceramic. (A) Fluorescent micrographs of HUVECs stained for filamentous actin. (B) The number of HUVECs adhered onto bare and DMA–MPC–PHB coated substrates after 2 days of culture. (C) Cell viability of HUVECs co-cultured with the bare and DMA–MPC–PHB coated substrates for 2 days. Data are presented as mean ± SD and analysed by T-test, *p < 0.05 (DMA–MPC–PHB coated samples vs. bare surface).

Blood adhesion resistance of DMA–MPC–PHB coating

For implantable biomedical devices with blood contacts such as cardiac catheters, blood adhesion resistance is an essential property. (27,28) In this regard, we further determined the anti- blood adhesion ability of the DMA–MPC–PHB coating by immersing each sample into whole blood for 2 minutes to evaluate the rapid blood contact adhesion, and incubating each sample with platelet-rich plasma (PRP) for 1 hour to observe

the platelet adhesion (29,30) After a 2-minute initial contact period, blood covered all bare substrates, but just a trace of blood adhered onto the DMA–MPC–PHB-4 coated substrates (Fig. 6A). After washing all substrates with deionized water and collecting the washing solution, we clearly observed that the color of the washing solution of the bare substrates were significantly darker than the washing solution of the DMA–MPC–PHB-4 coated samples. After detecting the absorbance of the washing solution at 545 nm, we found that the absorbance of all bare substrate washing solution was 3 to 4 times higher than that of all DMA–MPC–PHB-4 coated substrates (Fig. 6B). In addition, after incubation with PRP for 1 hour, massive platelet adhesion, with total amount of 9.2×10^3, 8×10^3 and 8.9×10^3 per mm^2 was found on the bare 316L SS, PDMS and ceramic substrates (Fig. 6C). The SEM showed the adherent platelets on bare substrates had a spread dendritic pattern, indicating that platelets were in a highly activated state (Fig. 6D). By comparison, only a few scattered platelets remained spherical on the DMA–MPC–PHB-4 coated surfaces, which indicated that the DMA–MPC–PHB coating provided diverse sub- strates with excellent blood adhesion resistance property.
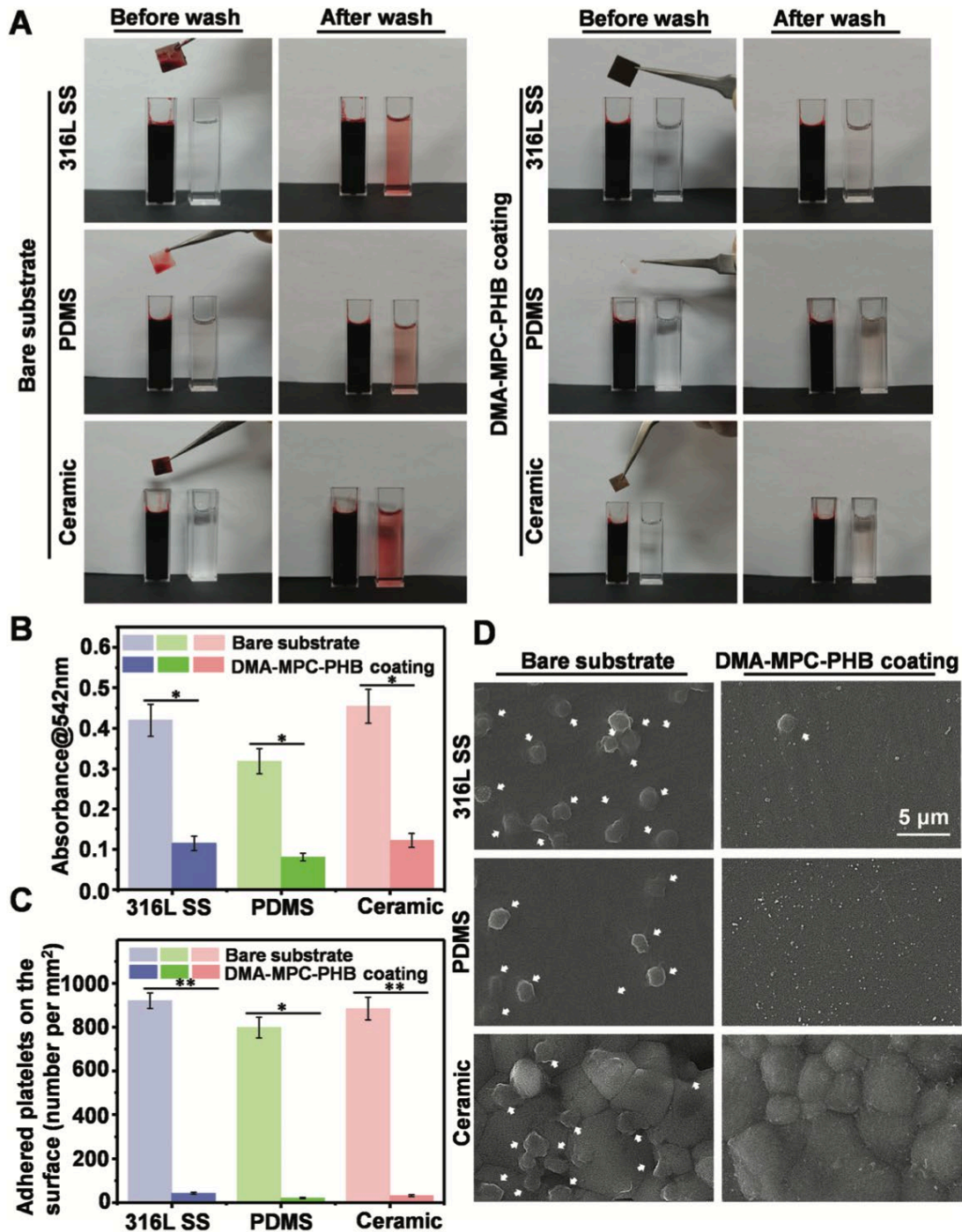
Fig. 6 Blood adhesion resistance of bare and DMA–MPC–PHB-coated 316L SS/PDMS/ceramic. (A) Images of bare (left) and DMA–MPC–PHB- coated (right) 316L SS/PDMS/ceramic substrates after 2-minute immersion in whole blood. (B) Absorbance of washing solution of each sample after 2-minute contact with blood. (C) SEM images of the platelets adhered onto bare and DMA–MPC–PHB-coated 316L SS/PDMS/ceramic. The adhered platelets are marked by white arrows. (D) Quantification of the platelets adhered on the different substrates, which was the average count of three SEM images randomly selected from each specimen. Data are presented as mean $\pm$ SD and analysed by T-test, *p < 0.05, **p < 0.01 (DMA–MPC– PHB coated samples vs. bare surface).

Conclusion

Physical lubrication and chemical antibacterial molecules are often dissociated when developing coatings for biomedical implants; (31,32) a single antibacterial mechanism is usually ineffective due to complicated

bacteria formation mechanism. In this study, we develop a biocompatible and multi-functional DMA–MPC–PHB coating, made of a universal adherent material DMA, a lubricating zwitterionic polymer MPC and an anti-bacteria molecule PHB. The DMA–MPC–PHB coating can adhere to a wide range of material surfaces (e.g., metal, polymer and ceramic) to simultaneously enhance the surface lubrication, inhibit bacterial adhesion and blood coagulation. The COF of the DMA–MPC–PHB coating was significantly reduced by about 40% compared to the bare surface. Due to the enhanced lubricating property, the DMA–MPC–PHB coating shows significant anti-bacterial ability (*E. coli* inhibition rate: 97.3%), while maintaining a cell viability over 90%. Moreover, the platelet adhesion and activation on the DMA–MPC–PHB surface are significantly decreased. As the DMA–MPC–PHB coating can be easily fabricated to modify a variety of substrate materials with improved lubrication as well as antibacterial ability, this strategy may serve as a universal surface modification strategy of implantable medical devices such as cardiovascular stents, cardiac/ urinary catheters and implantable defibrillator.

Materials and methods

Materials

316L SS sheets were purchased from Bochuang Metal Co., Ltd, China. PDMS prepolymer (SYLGARD® 184) was provided by Dow Corning, USA. Nearly inert bioceramic sheets (Zirconia, ZrO2) were provided by Qianen Co., Ltd, China. DMA was purchased from Kaiwei chemical Co., Ltd, China. MPC (98%) was purchased by Joy-Nature Co., Ltd, China. Poly(3-hydroxybuty- rate) (PHB) powder was obtained from Tian An Biologic Materials Co., Ltd, China. AIBN, and Tris-HCl buffer were from Aladdin Bio-Chem Technology Co., Ltd, China.

Synthesis of PHB

Antibacterial PHB was previously synthesized by our group. (19) Briefly, beta-butyrolactone (10 mmol), aluminum isopropoxide (1 mmol) and pyridine (2 mL) were firstly mixed and stirred under nitrogen (N2) at 65 °C for 48 hours, then the reaction was quenched by hydrochloric acid solution (2 M). Afterwards, dichloromethane (DCM, 20 mL) was added into the above reaction system for 3 times to extract the reaction products. The mixture solution was then subject to a rotary evaporation to remove the DCM. Finally, light-yellow PHB oligomer oil was obtained by eluting the residue with DCM/n-hexane (5 : 1, v : v) in a silica gel column.

Synthesis of DMA–MPC–PHB terpolymer

We then synthesized the terpolymer DMA–MPC–PHB by free radical polymerization. DMA, MPC, and PHB were dissolved separately in N,N-dimethylformamide (DMF) (50 mL) with different mass ratios of 1:1:1, 1:1:2, 1:2:1 and 1:2:2 (total weight: 1 g) under N2 atmosphere. After adding AIBN (initiator) (5 mg), the solution was stirred at 68 °C for 24 hours. Then the mixture was dialyzed with deionized water and freeze-dried to obtain the terpolymer DMA–MPC–PHB. The synthetic terpolymer was analyzed by attenuated total reflectance Fourier transform infrared spectroscopy (ATR-FTIR, Thermo Scientific NEXSA).

Fabrication and characterization of DMA–MPC–PHB-coated surfaces

To verify the DMA–MPC–PHB was a universal coating for surface functionalization, bare 316L SS, PDMS and Zirconia ceramic sheets were used as base materials. All bare 316L SS, PDMS and ceramic sheets were ultrasonically washed in acetone and deionized water for 30 minutes. The DMA–MPC– PHB terpolymer solution was dissolved at a concentration of 4 mg mL^{-1} in a Tris-DMF buffer (20% DMF, pH = 8.5).(33) The bare substrates were immersed in the terpolymer solutions at room temperature for 24 hours in dark.

Afterwards, the samples were soaked in 20 mg mL^{-1} sodium hydroxide (NaOH) for 10 minutes at room temperature to obtain hydroxylated surfaces. Then, the sheets were rinsed with deionized water and dried under vacuum, and the DMA–MPC– PHB coated samples were prepared. ^{1}H nuclear magnetic resonance (NMR) spectra with deuterated chloroform (CDCl3) as the deuterium solvents at 25 °C on a Varian 500 MHz solid state spectrometer (Palo Alto, USA). Subsequently, ATR-FTIR was used to characterize the three types of terpolymer-coated substrates (the coatings were measured directly on the surface of each sample) with 650–4000 cm^{-1} recording range, 2 cm^{-1} resolution and 16 scans per test. The morphology of the DMA–MPC–PHB coating was observed using SEM (Tescan VEGA3, Czech Republic). The chemical composition of the DMA– MPC–PHB coated sheets was evaluated using an XPS (Thermo Scientific NEXSA) spectrometer with a 15 kV Mg Kα radiation source. The thickness of the terpolymer-coated samples was determined using XP-2 profiler (AMBios Inc. USA). The static WCA of the terpolymer-coated surfaces was measured using a sessile drop method by a contact angle goniometer (OCA-20, Dataphysics Instruments, Germany). (33)

Lubrication performance of DMA–MPC–PHB-coated surfaces

AFM (MFP-3D-SA, USA) was used in contact mode at room temperature to conduct the tribological test for 316L SS, 316L SS@DMA–MPC–PHB, PDMS, PDMS@DMA–MPC–PHB, ceramic, and ceramic@DMA–MPC–PHB. A polystyrene micro- sphere (diameter: 5 mm) was attached to the jut of the tipless silicon cantilever (TL-CONT, NanoWorld AG, Switzerland) using curing glue that had been exposed to ultraviolet (UV) light for 50 minutes. The cantilever's spring constant (KN: 0.2 N m^{-1}) was measured using the frequency calibration method, and the cantilever's lateral sensitivity was determined using the improved wedge calibration method. Normal force of 100–300 nN (equivalent to a contact pressure of 34.4–49.6 MPa) was used in the tribological test, with a scanning rate of 2 Hz, 20 mm-long sliding distances, and 20 × 20 mm scanning area. (33) Deionized water served as the lubricating medium. The COF value was calculated by COF = f/N (f represents frictional force, N refers to normal force). Three data points were used to calculate the COF value.

Bacterial inhibition of DMA–MPC–PHB-coated surfaces

E. coli (ATCC 22792) was grown overnight in Luria–Bertani (LB) broth, and then the bacterial suspension was diluted to 1 × 10^6 CFU mL^{-1} in LB broth. After sterilization under UV light for 1 hour, the samples (316L SS, 316L SS@DMA–MPC–PHB, PDMS, PDMS@DMA–MPC–PHB, ceramic and ceramic@DMA–MPC–PHB) were placed in a 24-well plate and 1 mL of bacteria suspension was added into each well. Afterwards, all samples were incubated in an aerobic incubator at 37 °C for 24 hours. After 24-hour of incubation, the bacterial suspension was aspi- rated, and the samples were washed three times with PBS and fixed overnight at 4 °C by 2.5% glutaraldehyde. Subsequently, the samples were sequentially dehydrated with a series of graded ethanol solutions (30%, 50%, 70%, 90% and 100%). Finally, after gold spray treatment, the surface coating of the samples was examined by SEM to observe their resistance characteristics to bacteria. Meanwhile, another group of samples incubated for 24 hours was washed three times with PBS and blotted dry with absorbent paper. The samples were placed in sterile tubes with the addition of 500 μL LB broth to each tube and then vortex shaken for 1 minute to detach the bacteria from the surface of the samples. The samples were then removed and washed again with 500 μL LB broth. The antibacterial performance of the terpolymer coating was quantitatively evaluated using the spread plate method.34 Briefly, 100 μL of bacterial suspension in LB was added into LB agar plates in triplicate and then incubated at 37 °C overnight. Colonies from each plate were counted to calculate the anti- bacterial rate of the DMA–MPC–PHB coating.

Cell adhesion and cytocompatibility of DMA–MPC–PHB-coated surfaces

HUVECs were utilized to examine the cell adhesion on the DMA–MPC–PHB coating. HUVECs were cultured in endothelial cell growth media with 15% fetal bovine serum (FBS). The cells were digested by a trypsin-EDTA solution (0.25 wt%). All cultures were supplemented with 100 U mL^{-1} streptomycin and penicillin in an atmosphere of 5% CO2 at 37 °C. HUVEC suspension at the density of 2×104 cells per mL was seeded onto the substrates (316L SS, 316L SS@DMA–MPC–PHB, PDMS, PDMS@DMA–MPC–PHB, ceramic and ceramic@DMA–MPC– PHB), the area of each sample was same as the aperture (2 cm^2) of the 24-well culture plate. After culture for 1 hour and 2 days, cells were stained with Alexa Fluor 488 phalloidin (Thermo Fisher Scientific), and cell adhesion was examined by an upright fluorescence microscope (Nikon, Japan). Then the amount of the cells adhered to the coated surfaces was quantified by an automated cell counter (Countess II FL, Thermo Fisher Scientific). To verify the DMA–MPC–PHB coating is non- toxic to cells, cell viability was further evaluated. Briefly, HUVECs were seeded in a 24-well plate at the density of 2×10^4 cells per well and incubated for 6 hours to ensure the cells adhered to the wall. Afterwards, bare and coated samples were immersed into the medium and co-cultured with cells for another 48 hours. Cell viability was measured by the Cell Counting Kit-8 assay.

Blood adhesion of DMA–MPC–PHB-coated surfaces

Fresh blood from healthy Sprague Dawley rats (male, 300–400 g) was utilized for whole blood adhesion and platelet adhesion tests. Blood collection was conducted in accordance with protocols approved by the Ethics Committee of The Hong Kong Polytechnic University (18-19/70-BME-R-GRF). For the instant whole blood adhesion test, the substrates were sub- merged in whole blood for 2 minutes and then removed and photographed immediately. (34) Then, all substrates (316L SS, 316L SS@DMA–MPC–PHB, PDMS, PDMS@DMA–MPC–PHB, ceramic, and ceramic@DMA–MPC–PHB) were rinsed with de- ionized water (2 mL) in separate cuvettes to remove the adher- ent blood cells on the sample surface. Afterwards, the washing solution was transferred into new cuvette and the absorbance at 545 nm was measured with an UV spectrophotometer. For the platelet adhesion assay, fresh whole blood was centrifuged at 1500 rpm for 15 minutes to obtain the PRP. The PRP was added to the sample surfaces and incubated for 1 hour at 37 °C. After washing with PBS for three times, the adhered platelets were preserved with 2.5% glutaraldehyde solution overnight at 4 °C. Subsequently, the samples were taken out, dehydrated in increasing ethanol concentrations (30, 50, 70, 90, and 100%). Finally, all samples were coated with gold to perform SEM to analyze the platelet morphology.

Statistical analysis

All experiments were done in triplicate unless otherwise stated. The information was given in the form of a mean and standard deviation (SD). Statistical analysis was carried out by T-test and one-way ANOVA by applying Origin 8.0 software. $p < 0.05, 0.01$, and 0.001 were considered a statistically significant difference and remarked with *, **, ***, respectively.

Author contributions

X. Z. supervised the whole project. X. Z., H. Y. Z., H. M. L. and X. M. T. revised the manuscript. D. S. performed experiments. D. S. and J. D. R. analyzed the data and wrote the manuscript. H. M. W. did the lubrication evaluation. Z. H. Z. synthesized the PHB. All authors approved this paper for publication.

Conflicts of interest

The authors declare no conflict of interest.

Notes and references

1 A. J. T. Teo, A. Mishra, I. Park, Y. J. Kim, W. T. Park and Y. J. Yoon, Polymeric Biomaterials for Medical Implants and Devices, ACS Biomater. Sci. Eng., 2016, 2(4), 454– 472.

2 L. Yi, K. Xu, G. Xia, J. Li, W. Li and Y. Cai, New protein- resistant surfaces of amphiphilic graft copolymers contain-

ing hydrophilic poly(ethylene glycol) and low surface energy fluorosiloxane side-chains, Appl. Surf. Sci., 2019, 480, 923–933.

3 S. Veerachamy, T. Yarlagadda, G. Manivasagam and P. K. Yarlagadda, Bacterial adherence and biofilm for- mation on medical implants: a review, Proc. Inst. Mech. Eng., Part H, 2014, 228(10), 1083–1099.

4 K. Zheng, M. I. Setyawati, D. T. Leong and J. Xie, Antimicrobial Gold Nanoclusters, ACS Nano, 2017, 11(7), 6904–6910.

5 Y. Liu, X. Xia, L. Xu and Y. Wang, Design of hybrid beta- hairpin peptides with enhanced cell specificity and potent anti-inflammatory activity, Biomaterials, 2013, 34(1), 237– 250.

6 I. Zhuk, A. B. Attygalle, Y. Wu, M. R. Libera and S. A. Sukhishvili, Self-Defensive Layer-by-Layer Films with Bacteria-Triggered Antibiotic Release, ACS Nano, 2014, 8(8), 7733–7745.

7 J. Rao, Y. Yang, H. P. Bei, C. Y. Tang and X. Zhao, Antibacterial nanosystems for cancer therapy, Biomater. Sci., 2020, 8(24), 6814–6824.

8 M. Barnes, C. Feit, T. A. Grant and E. J. Brisbois, Antimicrobial polymer modifications to reduce microbial bioburden on endotracheal tubes and ventilator associated pneumonia, Acta Biomater., 2019, 91, 220–234.

9 T. Ron, K. P. Jacobsen and S. Lee, A catheter friction tester using balance sensor: Combined evaluation of the effects of mechanical properties of tubing materials and surface coatings, J. Mech. Behav. Biomed. Mater., 2018, 84, 12–21.

10 Q. Yu, Z. Wu and H. Chen, Dual-function antibacterial sur- faces for biomedical applications, Acta Biomater., 2015, 16, 1–13.

11 S. B. Goodman, J. Gallo, E. Gibon and M. Takagi, Diagnosis and management of implant debris-associated inflammation, Expert Rev. Med. Devices, 2020, 17(1), 41–56.

12 S. Jahn, J. Seror and J. Klein, Lubrication of Articular Cartilage, Annu. Rev. Biomed. Eng., 2016, 18, 235–258.

13 Y. Wang, W. Cui, X. Zhao, S. Wen, Y. Sun, J. Han and H. Zhang, Bone remodeling-inspired dual delivery electro- spun nanofibers for promoting bone regeneration, Nanoscale, 2018, 11(1), 60–71.

14 H. Chen, T. Sun, Y. Yan, X. Ji, Y. Sun, X. Zhao, J. Qi, W. Cui, L. Deng and H. Zhang, Cartilage matrix-inspired bio- mimetic superlubricated nanospheres for treatment of osteoarthritis, Biomaterials, 2020, 242, 119931.

15 X. Ji, Y. Yan, T. Sun, Q. Zhang, Y. Wang, M. Zhang, H. Zhang and X. Zhao, Glucosamine sulphate-loaded dis- tearoyl phosphocholine liposomes for osteoarthritis treat- ment: combination of sustained drug release and improved lubrication, Biomater. Sci., 2019, 7(7), 2716–2728.

16 L. Cheng, Y. Wang, G. Sun, S. Wen, L. Deng, H. Zhang and W. Cui, Hydration-Enhanced Lubricating Electrospun Nanofibrous Membranes Prevent Tissue Adhesion, Research, 2020, 2020, 4907185.

17 S. Jiang and Z. Cao, Ultralow-fouling, functionalizable, and hydrolyzable zwitterionic materials and their derivatives for biological applications, Adv. Mater., 2010, 22(9), 920–932.

18 C. Berne, C. K. Ellison, A. Ducret and Y. V. Brun, Bacterial adhesion at the single-cell level, Nat. Rev. Microbiol., 2018, 16(10), 616–627.

19 L. Ma, Z. Zhang, J. Li, X. Yang, B. Fei, P. H. M. Leung and X. Tao, A New Antimicrobial Agent: Poly (3-hydroxybutyric acid) Oligomer, Macromol. Biosci., 2019, 19(5), e1800432.

20 X. Lin, X. Fan, R. Li, Z. Li, T. Ren, X. Ren and T.-S. Huang, Preparation and characterization of PHB/PBAT-based bio- degradable antibacterial hydrophobic nanofibrous mem- branes, Polym. Adv. Technol., 2018, 29(1), 481–489.

21 Q. Tu, X. Zhao, S. Liu, X. Li, Q. Zhang, H. Yu, K. Xiong, N. Huang and Z. Yang, Spatiotemporal dual-delivery of therapeutic gas and growth factor for prevention of vascu- lar stent thrombosis and restenosis, Appl. Mater. Today, 2020, 19, 100546.

22 S. Hong, Y. S. Na, S. Choi, I. T. Song, W. Y. Kim and H. Lee, Non-Covalent Self-Assembly and Covalent Polymerization Co-Contribute to Polydopamine Formation, Adv. Funct. Mater., 2012, 22(22), 4711–4717.

23 J. Klein, Hydration lubrication, Friction, 2013, 1(1), 1–23.
24 J. Yang, Y. Han, J. Lin, Y. Zhu, F. Wang, L. Deng, H. Zhang, X. Xu and W. Cui, Ball-Bearing-Inspired Polyampholyte- Modified Microspheres as Bio-Lubricants Attenuate Osteoarthritis, Small, 2020, 16(44), e2004519.

25 S. Renvert, C. Lindahl, H. Renvert and G. R. Persson, Clinical and microbiological analysis of subjects treated with Branemark or AstraTech implants: a 7-year follow-up study, Clin. Oral Implants Res., 2008, 19(4), 342–347.
26 J. K. Woo, J. S. Webb, S. M. Kirov, S. Kjelleberg and S. A. Rice, Biofilm dispersal cells of a cystic fibrosis Pseudomonas aeruginosa isolate exhibit variability in functional traits likely to contribute to persistent infection, FEMS Immunol. Med. Microbiol., 2012, 66(2), 251–264.

27 Z. Yang, Y. Yang, L. Zhang, K. Xiong, X. Li, F. Zhang, J. Wang, X. Zhao and N. Huang, Mussel-inspired catalytic selenocystamine-dopamine coatings for long-term gene-ration of therapeutic gas on cardiovascular stents, Biomaterials, 2018, 178, 1–10.

28 F. Zhang, Q. Zhang, X. Li, N. Huang, X. Zhao and Z. Yang, Mussel-inspired dopamine-Cu(II) coatings for sustained in situ generation of nitric oxide for prevention of stent thrombosis and restenosis, Biomaterials, 2019, 194, 117– 129.

29 I. Banerjee, R. C. Pangule and R. S. Kane, Antifouling coatings: recent developments in the design of surfaces that prevent fouling by proteins, bacteria, and marine organ- isms, Adv. Mater., 2011, 23(6), 690–718.

30 W. Yang, H. Xue, W. Li, J. Zhang and S. Jiang, Pursuing "zero" protein adsorption of poly(carboxybetaine) from undiluted blood serum and plasma, Langmuir, 2009, 25(19), 11911–11916.

31 Q. Tu, X. Shen, Y. Liu, Q. Zhang, X. Zhao, M. F. Maitz, T. Liu, H. Qiu, J. Wang, N. Huang and Z. Yang, A facile metal–phenolic–amine strategy for dual-functionalization of blood-contacting devices with antibacterial and anti- coagulant properties, Mater. Chem. Front., 2019, 3(2), 265– 275.

32 T. Kang, X. Banquy, J. Heo, C. Lim, N. A. Lynd, P. Lundberg, D. X. Oh, H. K. Lee, Y. K. Hong, D. S. Hwang, J. H. Waite, J. N. Israelachvili and C. J. Hawker, Mussel- Inspired Anchoring of Polymer Loops That Provide Superior Surface Lubrication and Antifouling Properties, ACS Nano, 2016, 10(1), 930–937.

33 Y. Han, W. Zhao, Y. Zheng, H. Wang, Y. Sun, Y. Zhang, J. Luo and H. Zhang, Self-adhesive lubricated coating for enhanced bacterial resistance, Bioact. Mater., 2021, 6(8), 2535–2545.

34 W. Peng, P. Liu, X. Zhang, J. Peng, Y. Gu, X. Dong, Z. Ma, P. Liu and J. Shen, Multi-functional zwitterionic coating for silicone-based biomedical devices, Chem. Eng. J., 2020, 398, 125663.